Life Sciences 229 (2019) 187–199

Contents lists available at ScienceDirect

Life Sciences

journal homepage: www.elsevier.com/locate/lifescie

Hyperbaric oxygen therapy reduces apoptosis and dendritic/synaptic degeneration via the BDNF/TrkB signaling pathways in SCI rats

Xinwang Ying[a,b], Wenzhan Tu[a,b], Sisi Li[a,b], Qiaoyun Wu[a,b], Xiaolong Chen[a,b], Ye Zhou[a,b], Jie Hu[a,b], Guanhu Yang[b], Songhe Jiang[a,b,*]

[a] Department of Physical Medicine and Rehabilitation, The Second Affiliated Hospital and Yuying Children's Hospital, Wenzhou Medical University, Wenzhou 325000, Zhejiang Province, China
[b] Department of Intelligent Rehabilitation International (cross-strait) Alliance, Wenzhou Medical University, Wenzhou 325000, Zhejiang Province, China

ARTICLE INFO

Keywords:
Spinal cord injury
BDNF/TrkB
Apoptosis
Dendritic/synaptic degeneration
Hyperbaric oxygen therapy

ABSTRACT

Spinal cord injury (SCI) is a serious neurological disease without efficacious drugs. Anti-apoptosis and suppressing dendritic/synaptic degeneration in the anterior horn are essential targets after SCI. Previous studies found that hyperbaric oxygen therapy (HBOT) significantly protected rats after SCI. However, its potential effects and mechanisms remain unknown. The BDNF/TrkB signaling pathways evidently contribute to the SCI recovery. Currently, we mainly investigate the potential effects and mechanism of HBOT on anti-apoptosis and ameliorating impaired dendrites, dendritic spines and synapses after SCI. Establish SCI model and randomly divide rats into 5 groups. After SCI, rats were subjected to HBOT. ANA-12 is the specific inhibitor of BDNF/TrkB signal pathway. Changes in neurological deficit, neuronal morphology, apoptosis, protein expression and dendrite/synapse were examined by Basso–Beattie–Bresnahan (BBB) locomotor rating scale, Hematoxylin-eosin (HE) and Nissl staining, TUNEL staining, RT-PCR, Western blot, immunofluorescence and Golgi-Cox staining. We found HBOT suppressed dendritic/synaptic degeneration and alleviated apoptosis, consistent with the increase of BDNF and TrkB expression and improved neurological recovery. In contrast to the positive effects of HBOT, inhibitor increased degeneration and apoptosis. Moreover, we observed that these HBOT-mediated protective effects were significantly inhibited by inhibitor, consistent with the lower expression of BDNF/TrkB and worse neurobehavioral state. These findings suggest that hyperbaric oxygen therapy ameliorates spinal cord injury-induced neurological impairment by anti-apoptosis and suppressing dendritic/synaptic degeneration via upregulating the BDNF/TrkB signaling pathways.

1. Introduction

Spinal cord injury (SCI) represents a clinical and socioeconomic burden with an increasing incidence. Each year, 250,000 to 500,000 people worldwide suffer an SCI according to data from the WHO, although there are no effective and reliable cures [1]. SCI implicates both primary and secondary injury mechanisms that cause severe neurological dysfunction, including motor, sensory, and autonomic dysfunction [2,3]. However, surgery can only relieve spinal cord compression and restore spinal stability [4]. The use of methylprednisolone as a treatment option remains controversial [5]. Therefore, it is crucial to introduce a safe and effective treatment to prevent or reverse secondary damage.

In the anterior horn of the spinal cord, dendrites are a necessary condition for signal transmission, and dendritic spines are essential factors influencing the transmission of excitatory information. [6]. Moreover, the structure and density of dendritic spines indicate the efficiency of information integration from axons to dendrites, which

Abbreviations: SCI, spinal cord injury; HBOT, hyperbaric oxygen therapy; BDNF, brain-derived neurotrophic factor; TrkB, tyrosine-related kinase B; PSD, post-synaptic density; MAP-2, microtubule-associated protein-2; LTP, long-term potentiation; LTD, long-term depression; HDG, hippocampal dentate gyrus; ATA, atmosphere absolute; TEM, transmission electron microscopy; S, sham-operated; M, spinal cord injury model; HM, spinal cord injury model followed by 7-day hyperbaric oxygen therapy; IM, spinal cord injury model followed by intraperitoneal injection inhibitor; IHM, spinal cord injury model followed by hyperbaric oxygen therapy with intraperitoneal injection inhibitor; SH, sham-operated followed by 7-day hyperbaric oxygen therapy; SHI, sham-operated followed by 7-day hyperbaric oxygen therapy with intraperitoneal injection inhibitor

* Corresponding author at: Department of Physical Medicine and Rehabilitation, The Second Affiliated Hospital and Yuying Children's Hospital, Wenzhou Medical University, Wenzhou 325000, Zhejiang Province, China.
E-mail address: jshwz@126.com (S. Jiang).

https://doi.org/10.1016/j.lfs.2019.05.029
Received 19 March 2019; Received in revised form 6 May 2019; Accepted 10 May 2019
Available online 17 May 2019

plays a crucial role in motor function [7,8]. Dendritic spines provide a morphological basis for synaptic plasticity and most spines exhibit a single, continuous postsynaptic density (PSD) [7]. Additionally, PSD95 and SYN1 are pre- and post-synaptic marker proteins, respectively. Selectively located in the dendrites, MAP-2 is a marker protein of dendrites [9]. Normally, dendritic spine density is correlated to motor activity patterns [10]. After SCI, the neural circuit is deprived of supraspinal input, causing paralysis, neuronal apoptosis, dendritic retraction, dendritic atrophy and dendritic spine loss [11]. A previous study showed that the loss of dendrite processes occurs after SCI and is generally maintained weeks later without therapy [12].

Hyperbaric oxygen therapy (HBOT) is a low-cost treatment method with few side effects. A clinical retrospective study reported that HBOT has a great effect in acute SCI patients, and HBOT is beneficial to recovery in the early stage of acute SCI. [13]. Previous experiments have focused on the effects of HBOT, such as its ability to reduce neuro inflammation, oxidative stress, neuronal death and promote angiogenesis and axon regeneration following SCI [14]. However, there is limited information regarding its effects on the dendrite、dendritic spine and synapse in the anterior horn of the gray matter after SCI. Emerging evidence indicates that HBOT can promote the reconstruction of dendrites and the maturation of dendritic spines in the injured brain. Hyperbaric oxygen pretreatment significantly improved learning and memory ability through suppressing dendritic spine loss and reducing neuronal apoptosis [15]. Interestingly, the combination of 5-HT and bike therapy can restore dendritic density loss to facilitate locomotor recovery within the 7d post SCI [11]. After 7d SCI, whether the reduction of dendrites and synapse damage is the target for HBOT to promote functional recovery has not been documented. Thus, we assumed that HBOT could alleviate dendritic atrophy、reduce dendritic spine loss and inhibit synaptic degeneration after 7d SCI. HBOT significantly overcame neuronal apoptosis after SCI [16,17]. However, the potential mechanism of HBOT on anti-apoptosis after SCI remains to be elucidated.

Following SCI, BDNF is crucial for the survival and plasticity of neuronal populations. Additionally, the role that BDNF plays in spinal plasticity after SCI is unequivocally linked to changes in the expression and function of the BDNF receptor, TrkB [18–20]. Numerous studies showed that both BDNF and TrkB expression levels were significantly elevated in spinal cord lesions and reach maxima at 7 days after SCI [21]. BDNF has a positive role in affecting dendritic branching, dendritic spine morphology, synaptic plasticity and long-term potentiation (LTP) in rat brain slices [22–24]. Interestingly, BDNF plays an important role in shaping synaptic plasticity and defining the prognosis of locomotor performance after SCI [25]. Moreover, increase of BDNF in lumber motoneurons significantly suppresses dendritic atrophy and synaptic degeneration [26]. All of the above demonstrate that the BDNF/TrkB signaling pathway is closely related to inhibit the degeneration of dendrite、dendritic spine and synapse. In addition, BDNF/TrkB signaling is involved in regulating HBOT-induced neuroprotection in rat brains following traumatic injury [27]. However, whether HBOT can regulate the BDNF/TrkB signaling pathway to ameliorate locomotor function recovery after SCI by suppressing apoptosis and degeneration of dendrite and synapse in the anterior horn of the gray matter is unknown.

This study aimed to investigate the neuroprotective effects (alleviating apoptosis, dendrite and dendritic spine loss and reducing synaptic damage) of HBOT on SCI and the potential mechanism of HBOT on these effects. Using rat model of SCI, we found that HBOT suppressed dendritic/synaptic degeneration and alleviated apoptosis, with obvious increase in BDNF and TrkB expression and neurological recovery. We then intraperitoneally injected a specific inhibitor of BDNF/TrkB to test the hypothesis that HBOT can regulate the BDNF/TrkB signaling pathway to ameliorate locomotor function. In contrast to the protective effects of HBOT, inhibitor (ANA-12) increased degeneration and apoptosis. Moreover, we observed that these HBOT-mediated protective effects were significantly inhibited by ANA-12, same as the lower expression of BDNF/TrkB and neurobehavioral score. These findings suggest that hyperbaric oxygen therapy ameliorates spinal cord injury-induced neurological impairment by anti-apoptosis and suppressing dendritic/synaptic degeneration via upregulating the BDNF/TrkB signaling pathways.

2. Material and method

2.1. Reagents and antibodies

Anti-TrkB, anti-BDNF, anti- caspase 3, anti-MAP-2 and anti- β-tubulin were purchased from Proteintech (Rosemont, IL, USA). Anti-PSD95 was purchased from Abcam (330 Cambridge Science Park, Cambridge, UK). Anti-Bax and anti-Bcl-2 were purchased from Cell Signaling Technology (Danvers, MA, USA). The BDNF/TrkB inhibitor ANA-12 was purchased from Selleckchem (Houston, TX, USA). An FD Rapid GolgiStain Kit was purchased from FD NeuroTechnologies, Inc. (Guilford, MD, USA). In Situ Cell Death Detection Kit was purchased from Roche Molecular Biochemicals.

2.1.1. Animals

98 adult (8-week-old) Sprague-Dawley male rats weighing 200–250 g were purchased from Shanghai Laboratory Animal Center (Shanghai, China). All the experimental protocols were approved by the Animal Research Committee of Wenzhou Medical University and followed the National Institutes of Health Guide for the Care and Use of Laboratory Animals. All rats were maintained in separate cages, 55 ± 5% relative humidity, 22 ± 1 °C, 12: 12-h light/dark cycle, with free access to food and water. All rats were randomly divided into five groups: Sham-operated: (n = 16; group S); Spinal cord injury model (n = 16; group M); Spinal cord injury model followed by 7-day hyperbaric oxygen therapy (n = 16; group HM); Spinal cord injury model followed by intraperitoneal injection inhibitor (n = 16; group IM); Spinal cord injury model followed by hyperbaric oxygen therapy with intraperitoneal injection inhibitor (n = 16; group IHM); Sham-operated followed by 7-day hyperbaric oxygen therapy (n = 9; group SH); SHI, Sham-operated followed by 7-day hyperbaric oxygen therapy with intraperitoneal injection inhibitor (n = 9; group SHI).

2.2. Spinal cord injury model

Rats were anesthetized by an intraperitoneal (i.p.) injection of 2% sodium pentobarbital (30 mg/kg). Then rats' backs were shaved and a 15-mm midline skin incision was made. Using the New York University (NYU) Impactor to hit the exposed cord (10 g × 25 mm) except the S, SH and SHI groups. SCI model was evidenced in the SCI groups by observing the body trembled, the tail swayed and the lower limbs retracted. Then sutured the wound and disinfected it with alcohol. Emptied the urinary bladder manually twice a day after surgery.

2.3. Hyperbaric oxygen therapy and injection of the inhibitor (ANA-12)

At 6 h after surgery, rats in the HM, IHM, SH and SHI group were placed in a perforated squirrel cage and subjected to HBO intervention in a monoplace hyperbaric chamber (DS400-IV, Weifang Huaxin Oxygen Industro. Ltd., Shandong, Chiy Cna). Washed the chamber for 5 min with pure oxygen maintained the atmosphere absolute (ATA) at 2.0. Then, pure oxygen was added continuously for 90 min to maintain an oxygen concentration above 96.5%, followed by uniform decompression to an atmospheric pressure for 15 min [27–29]. Rats in the S, M and the IM group were placed inside the chamber but did not undergo HBOT.

After surgery, rats in IM, IHM and SHI group were intraperitoneally injected with inhibitor, ANA12 (0.5 mg/kg) every 24 h following SCI and an equal volume of saline was injected in S, M, HM and SH group.

Notably, ANA12 is stable in body fluids and can cross through the blood spinal cord barrier [30].

2.4. Locomotion tests

BBB locomotor rating scale was evaluated in an open field at 6 h, 1 d, 3 d, and 7 d post SCI [31]. Briefly, the BBB locomotion rating scale scores ranged from 0 point (complete paralysis) to 21 points (normal). The lower the score, the more serious the injury.

2.5. Tissue preparation and HE Nissl staining

28 rats in total were sacrificed after 7 d SCI. Briefly, under deep anesthesia with 2% sodium pentobarbital, rats were perfused with 0.9% saline, followed by 4% paraformaldehyde in 0.1 M phosphate buffer (PB, pH 7.4). The spinal cord tissue was then removed, kept in the same fixative for 24 h at 4 °C, and immersed in 0.1 M phosphate-buffered 30% sucrose overnight at 4 °C. Coronal sections (10 μm thick) of the spinal cord were cut.

HE staining used the hemalum. Hemalum dyes the nucleus blue and Eosin stains the cytoplasm into red. The step of Nissl staining was based on the steps in a previous report [32].

2.6. TUNEL staining

Prepared sections were collected for TUNEL staining. Permeabilized the slides for 10 min at room temperature and washed the slides three times for 15 min. Then we use an In Situ Cell Death Detection Kit to detect the apoptotic cells. Using Olympus microscope to collect the images. The apoptosis positive cells were counted quantitatively, with four animals examined per group and three slices per spinal cord sample.

2.7. Western blot analysis

The prepared spinal cord tissue samples were removed from −80 °C into fresh RIPA protein lysis buffer containing PMSF (RIPA: PMSF = 100:1) three times at 12,000 rpm for 5 min at 4 °C and subsequently collected the supernatant. Protein concentration of each sample was calculated using a BCA protein assay kit. Then the protein was mixed with loading buffer, heated to 100 °C for 10 min and separated on a 10% or 12% Tris–HCl SDS-PAGE gel (Bio-Rad, Hercules, CA). After electrophoresis, the blots were sequentially incubated with primary and secondary antibodies. Signals were digitally quantified using a UVP gel-imaging system (Upland, CA, USA) and analyzed using AlphaEaseFC (version 4.0).

2.8. Immunofluorescence staining

Prepared slices were dried and washed using 0.1 M PBS (pH 7.6) twice for 10 min. After treatment with 10% normal non-immune goat serum for 1 h, sections were incubated first with primary antibodies overnight. Followed by Alexa Fluor 488 Affinipure Goat anti-Rabbit IgG (H + L) for 1 h. Sections were washed three times with PBS, incubated with DAPI for 10 min, and finally washed in PBS and sealed with a coverslip. Fluorescent signals were observed under a fluorescence microscope (BX51, Olympus). The number of positive cells per section was calculated, with four animals examined per group and three slices per spinal cord sample.

2.9. RT-PCR

The primer sequences were 5′ CTGGGGCTTATGCTTGCTGGT 3′ (Forward), 5′TGATGTTCTCTGGGTCAATGCTGTT 3′ (Reverse) for TrkB, 5′TCTACGAGACCAAGTGTAATCCCAT 3′ (Forward), 5′GAAGTGTCTAT CCTTATGAACCGC 3′ (Reverse) for BDNF. High Capacity RNA-to-cDNA Master Mix (A3500, Promega) was applied to reverse transcribed the one microgram of total RNA. Real-time amplification was performed using SYBR Green Supermix and a Light Cycler480. The PCR reactions were prepared in a total volume of 10 μl containing 1 μl diluted RNA, 0.5 μl forward and 0.5 μl reverse primer, 5 μl 2× SYBR® Green Reaction Mix, and 3 μl RNase-free water. To amplify genomic DNA, PCR was performed under the following conditions: reverse transcription at 50 °C for 3 min, DNA polymerase activation and RT enzyme inactivation at 95 °C for 5 min, followed by 45 cycles of denaturation at 95 °C for 10 s, primer annealing at 60 °C for 10 s, and elongation at 72 °C for 10 s. Comparative mRNA expression levels were expressed as $2^{-\Delta\Delta Ct}$.

2.10. Transmission electron microscopy

Fresh spinal cord tissues were isolated from the anterior horn without heart perfusion. Then the tissues were quickly cut into $1mm^3$ size and soaked in 2.5% glutaraldehyde. Tissues were washed in PBS three times for 15 min. Following fixation in 1% osmic acid for 1 h, spinal cord tissues were stained with 1% uranyl acetate for 2 h. After dehydrating with gradient acetone solution, spinal cord tissues were embedded for coronal sections. Following location by semi-thin section and toluidine blue staining, the tissues were cut into ultrathin sections and finally observed using a Hitachi TEM.

2.11. Golgi staining

Briefly, the fresh spinal cord samples were immersed in impregnation solution (mixture of solution A and B = 1:1) and darkly stored at room temperature for 2 weeks. The samples were then transferred to impregnation solution C and darkly kept for 48 h at 4 °C. Afterward, they were sliced using a horizon sliding slicer at a thickness of 150 μm and stained using standard staining procedures.

2.12. Sholl analysis

Neurons within the anterior horn of T9-T11 were traced at 400× magnification. To measure the length of dendrites, Sholl analysis [33] was conducted using a Sholl analysis plug-in for ImageJ software. The number of intersections of dendrites with a series of concentric rings at 10 μm intervals from the center of the cell body was counted for each cell. The total dendritic length was determined by multiplying the number of intersections by 10 μm [34]. Five neurons were selected from each group and compared using one-way analysis of variance (ANOVA).

2.13. Measurement of spine density

Dendritic spine density was analyzed in T9-T10 neurons within the anterior horn. Each cell was traced at 400× magnification. The number of dendrites and the length of the dendrites were calculated to yield spines/μm data [35]. We did not make any attempt to correct for spines hidden by overlying dendrites. Therefore, the data may underestimate the actual spine density.

2.14. Statistical analysis

Data were presented as the mean ± SD. Statistical significance was examined using Student's *t*-test when there were two experimental groups. When more than two groups were compared, statistical evaluation of the data was performed using one-way analysis of variance (ANOVA) and Dunnett's post hoc test. Statistical analyses were carried out using the SPSS.16 statistical software and p values < 0.05 were considered statistically significant.

Table 1
Comparison of BBB scores of rats in different groups at different time points ($\bar{x}$ ± SD).

Groups	n	6 h	1 day	3 days	7 days
S	16	21.00 ± 0.00	21.00 ± 0.00	21.00 ± 0.00	21.00 ± 0.00
SH	9	21.00 ± 0.00	21.00 ± 0.00	21.00 ± 0.00	21.00 ± 0.00
SHI	9	21.00 ± 0.00	21.00 ± 0.00	21.00 ± 0.00	21.00 ± 0.00

Table 2
Comparison of BBB scores of rats in different groups at different time points ($\bar{x}$ ± SD).

Groups	n	6 h	1 day	3 days	7 days
S	16	21.00 ± 0.00	21.00 ± 0.00	21.00 ± 0.00	21.00 ± 0.00
M	16	0.00 ± 0.00$^{\#}$	1.70 ± 0.45$^{\#}$	2.70 ± 0.67$^{\#}$	5.22 ± 0.75$^{\#}$
HM	16	0.00 ± 0.00	2.20 ± 0.84	3.30 ± 0.57	6.56 ± 0.39*
IM	16	0.00 ± 0.00	1.00 ± 0.61	2.10 ± 0.89	3.94 ± 0.46$^{\Delta}$
IHM	16	0.00 ± 0.00	1.80 ± 0.76	2.90 ± 0.65	5.56 ± 0.63$^{\&}$

Data were presented as mean ± SD, $^{\#}p < 0.05$ as compared to the S , $^{*}p < 0.05$ as compared to the M, $^{\Delta}$ $p < 0.05$ as compared to the M, $^{\&}$ $p < 0.05$ as compared to the HM.

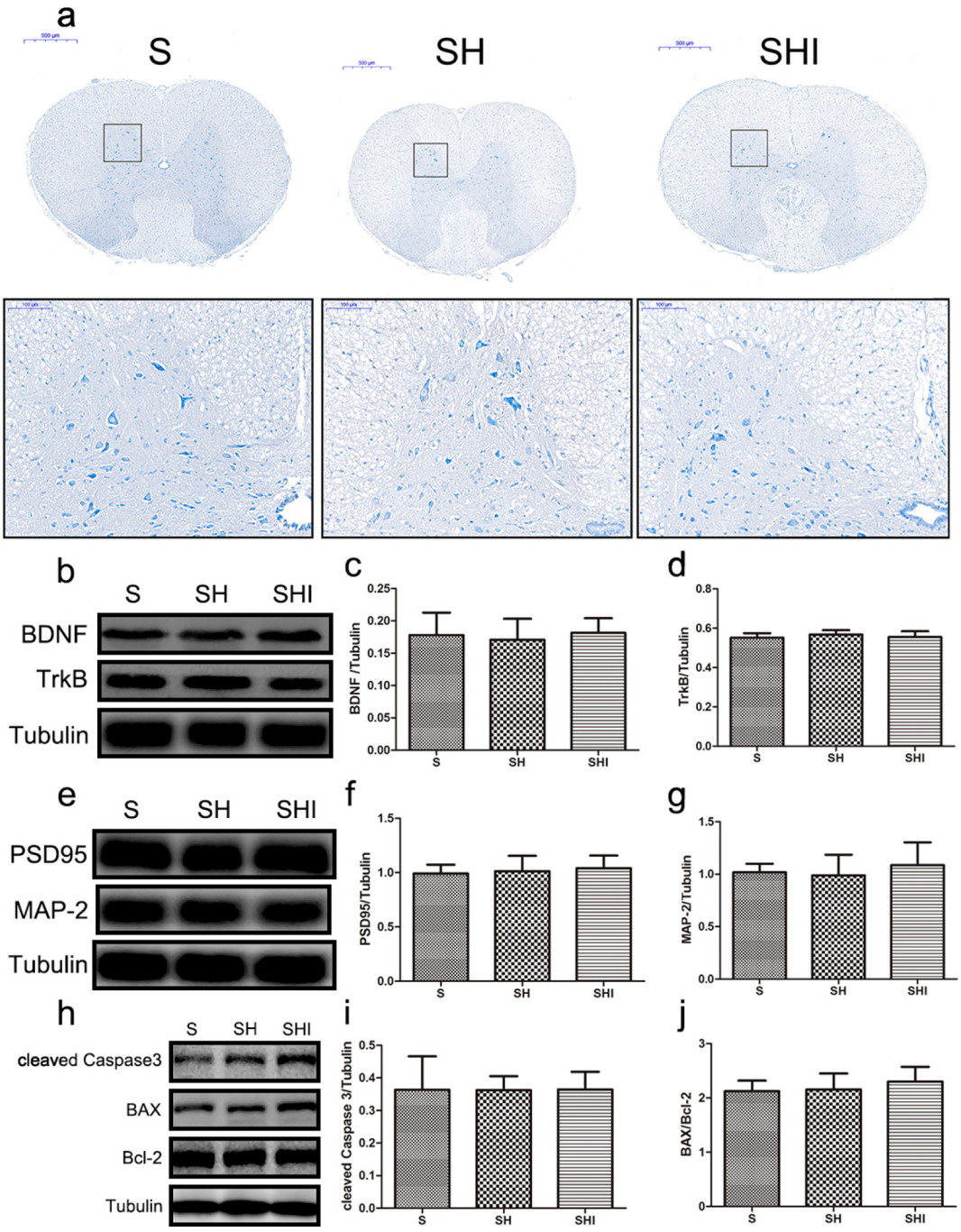

Fig. 1. HBOT had no significant effects on the BDNF/TrkB signaling pathway as well as BBB scores, tissue structure and protein expression in the S group. a. Nissl staining. Scale bars are 500 μm and 100 μm, respectively. b, c, d, e, f, g, h, I, j Represent western blots and quantification data of BDNF/Tubulin, TrkB/Tubulin, PSD95/Tubulin, MAP-2/Tubulin, cleaved Caspase3/Tubulin and BAX/Bcl-2 in each group. Columns represent mean ± SD, $n = 5$.

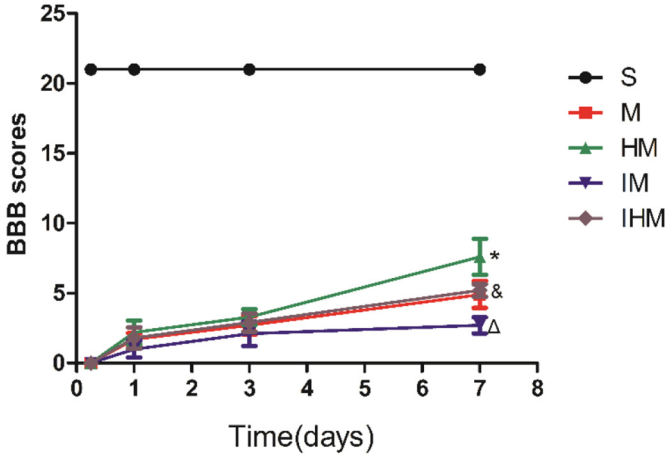

Fig. 2. BBB scores in different groups.

3. Results

3.1. HBOT had no significant effects on the BDNF/TrkB signaling pathway as well as BBB scores, tissue structure and protein expression in the S group

The BBB scores in the three groups were all 21 (normal) (Table 1). According to the Nissl staining, there were no observable pathological changes among the three groups (Fig. 1a).

We detected whether HBOT can affect the expression level of BDNF/TrkB signaling pathway and HBOT can play roles through the BDNF/TrkB signaling pathway in the S group. Compared with SH group, the expression of BDNF and TrkB in both S and SHI group were no statistical difference (S vs. SH; SH vs. SHI: $p > 0.05$) (Fig. 1b, c, d).

We further tested whether HBOT can regulate dendritic and synaptic-related protein (PSD95 and MAP2) as well as apoptosis-related protein (cleaved Caspase3 and BAX/Bcl-2) expression levels. Compared with S group, the expression changes of PSD95, MAP-2, cleaved Caspase3 and BAX/Bcl-2 in the SH groups were not obvious ($p > 0.05$). Additionally, consistent with the comparison results between the S group and the SH group, the difference of these protein expression level between the SH group and the SHI group was also not statistically significant. ($p > 0.05$) (Fig. 1e, f, g, h, i, j).

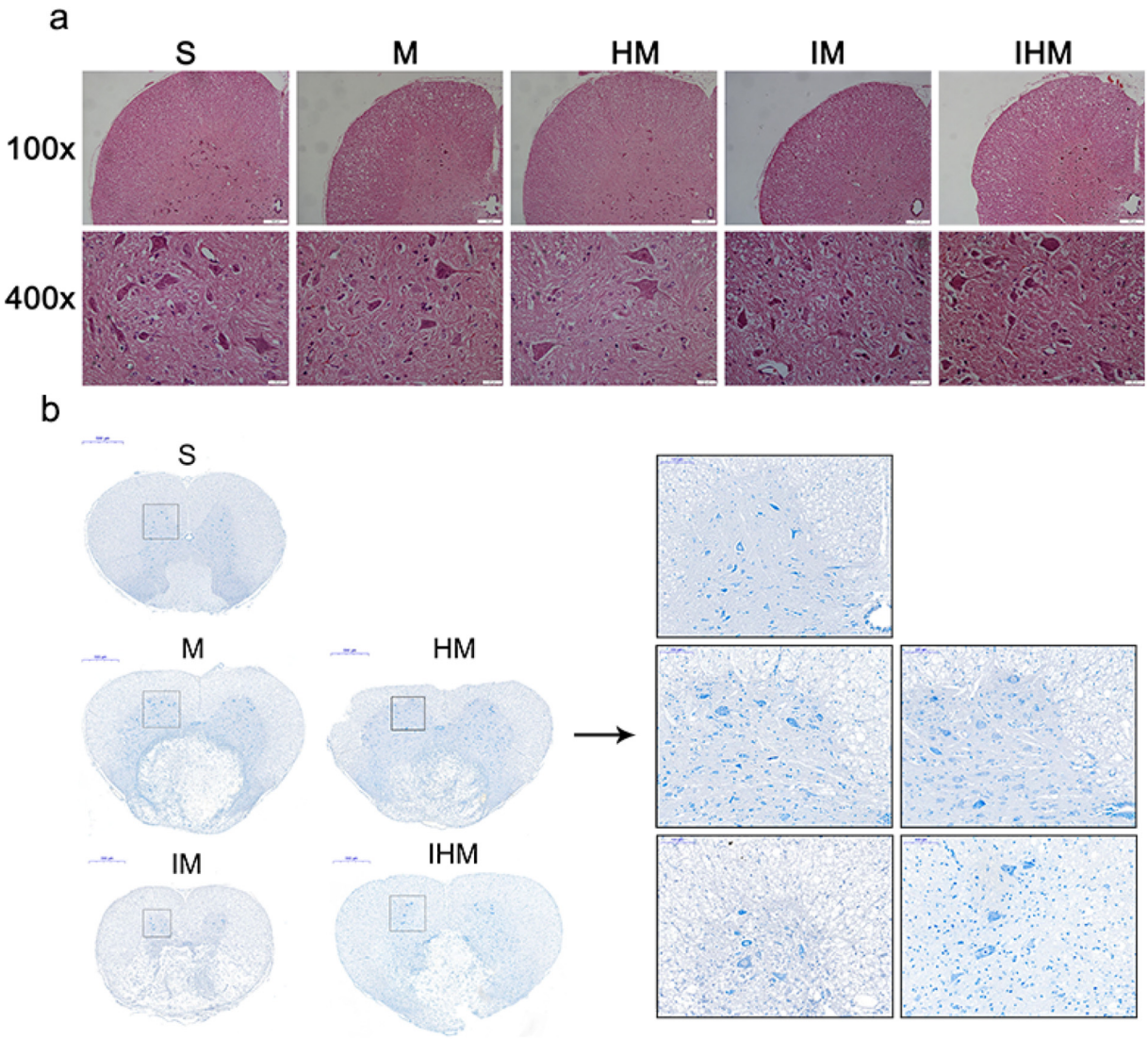

Fig. 3. HBOT ameliorated tissue structure damage in the anterior horn after SCI, while the inhibitor had the opposite effects. a HE staining at 7 days after SCI. Scale bars are 100 μm and 20 μm, respectively. b Nissl staining to observe the change of neural Nissl body at 7 days after SCI. Scale bars are 500 μm and 100 μm, respectively.

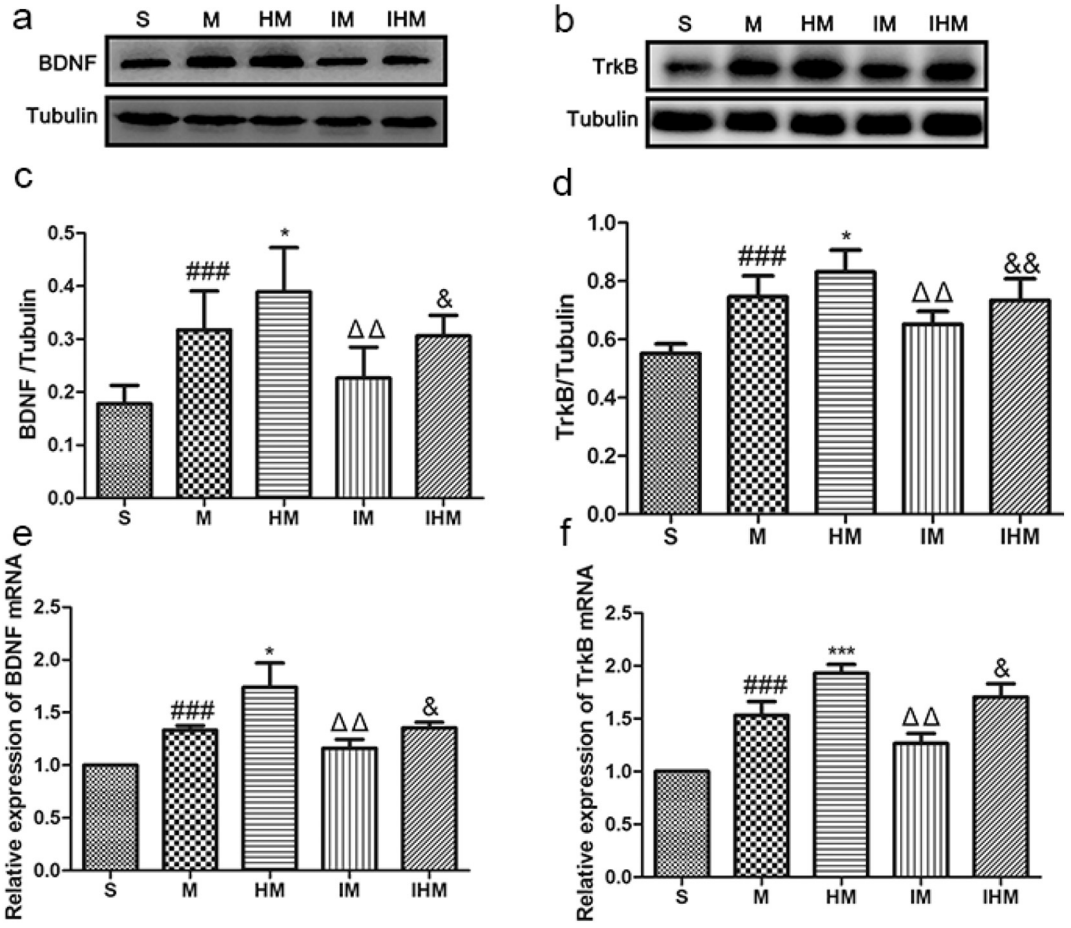

Fig. 4. HBOT upregulated the BDNF/TrkB signaling pathway following SCI, while inhibitor decreased the HBOT-dependent BDNF/TrkB signaling pathway. a, b, c, d Represent western blots and quantification data of BDNF/Tubulin and TrkB/Tubulin in each group; columns represent mean ± SD, $n = 5$. e, f Represent RT-qPCR analysis of BDNF and TrkB mRNA expression at 7 days in different groups. Columns represent mean ± SD, n = 5. $^{\#}p < 0.05$ as M group versus S group, $^{*}p < 0.05$ as HM group versus M group, $^{\Delta}p < 0.05$ as IM group versus M group, $^{\&}p < 0.05$ as IHM group versus HM group. ($^{\#}p$, $^{*}p$, $^{\Delta}p$, $^{\&}p < 0.05$; $^{\#\#}p$, $^{**}p$, $^{\Delta\Delta}p$, $^{\&\&}p < 0.01$; $^{\#\#\#}p$, $^{***}p$, $^{\Delta\Delta\Delta}p$, $^{\&\&\&}p < 0.001$).

3.2. HBOT decreased tissue structure damage in the anterior horn and improved functional recovery after SCI, while the inhibitor had the opposite effects

We evaluated BBB scores at 6 h, 1 day, 3 days and 7 days after SCI. According to the BBB scores, the motor function of the S group was normal (Table 2, Fig. 2). There was no significant difference in BBB scores among the other four groups at 6 h and 1 day after SCI ($p > 0.05$). The M group showed a remarkably decreased BBB scores at both 3 days and 7 days compared with the S group ($p < 0.001$). Rats in the HM group had significantly higher scores than those in the M group at 7 days (HM vs. M, $p = 0.0047$). Compared with the M group, the IM group exhibited a significantly worse motor function at 7 days (IM vs. M, $p = 0.0072$). In addition, the IHM group showed a remarkably lower BBB score than the HM group at 7 days (IHM vs. HM, $p = 0.013$). Similarly, the change in the trend of the BBB scores at 3 days was consistent with that at 7 days, but there was no significant difference among the four SCI groups ($p > 0.05$). Additionally, BBB scores of M group at 7 days were remarkably higher than these at 6 h after SCI ($p < 0.001$), indicating that there was a gradual self-recovery process.

Histomorphological differences in the anterior horn of the T9-T11 level were observed by HE staining at 7 days after injury (Fig. 3a). There were no pathological structures in the S group, while severe damage of the gray matter in the anterior horn was evident in the M group relative to the S group. Rats in the HM group showed a more regular arrangement in anterior horn than that of rats in the M group and the IHM group. Changes in the IM group were more severe compared with those in the M group, with swollen cells, necrosis and apoptosis, enlarged intercellular space and disordered arrangement of the neurons, which were correlated with a significant decline in locomotor function. Nissl staining showed that the HM group had less motoneuron loss while the IM group had more motoneuron loss than the M group (Fig. 3b). Furthermore, the destruction of pathological structures in the IHM group was more severe than that in the HM group.

3.3. HBOT upregulated the BDNF/TrkB signaling pathway following SCI, while inhibitor downregulated the HBOT-dependent BDNF/TrkB signaling pathway

We used Western blot and RT-qPCR to analyze the total expression of BDNF and TrkB in the T9-T11 region. After normalization with β-tubulin, the results showed that the M group had remarkably upregulated expression levels of BDNF and TrkB compared with the S group (BDNF, M vs S, $p < 0.001$; TrkB, M vs S, $p < 0.001$) (Fig. 4a, b, c, d). BDNF and TrkB expression in the HM group was significantly increased but significantly decreased in the IM group compared with the M group (BDNF, HM vs M, $p = 0.034$; TrkB, HM vs M, $p = 0.016$; BDNF, IM vs M, $p = 0.009$; TrkB, IM vs M, $p = 0.008$). In terms of RT-qPCR analysis, there was also a significant difference in BDNF and TrkB mRNA expression levels between the M and HM groups (BDNF mRNA, HM vs M, $p = 0.023$; TrkB mRNA, HM vs M, $p < 0.001$) (Fig. 4e, f) and between the M and IM groups at 7 days after SCI (BDNF mRNA, IM vs M,

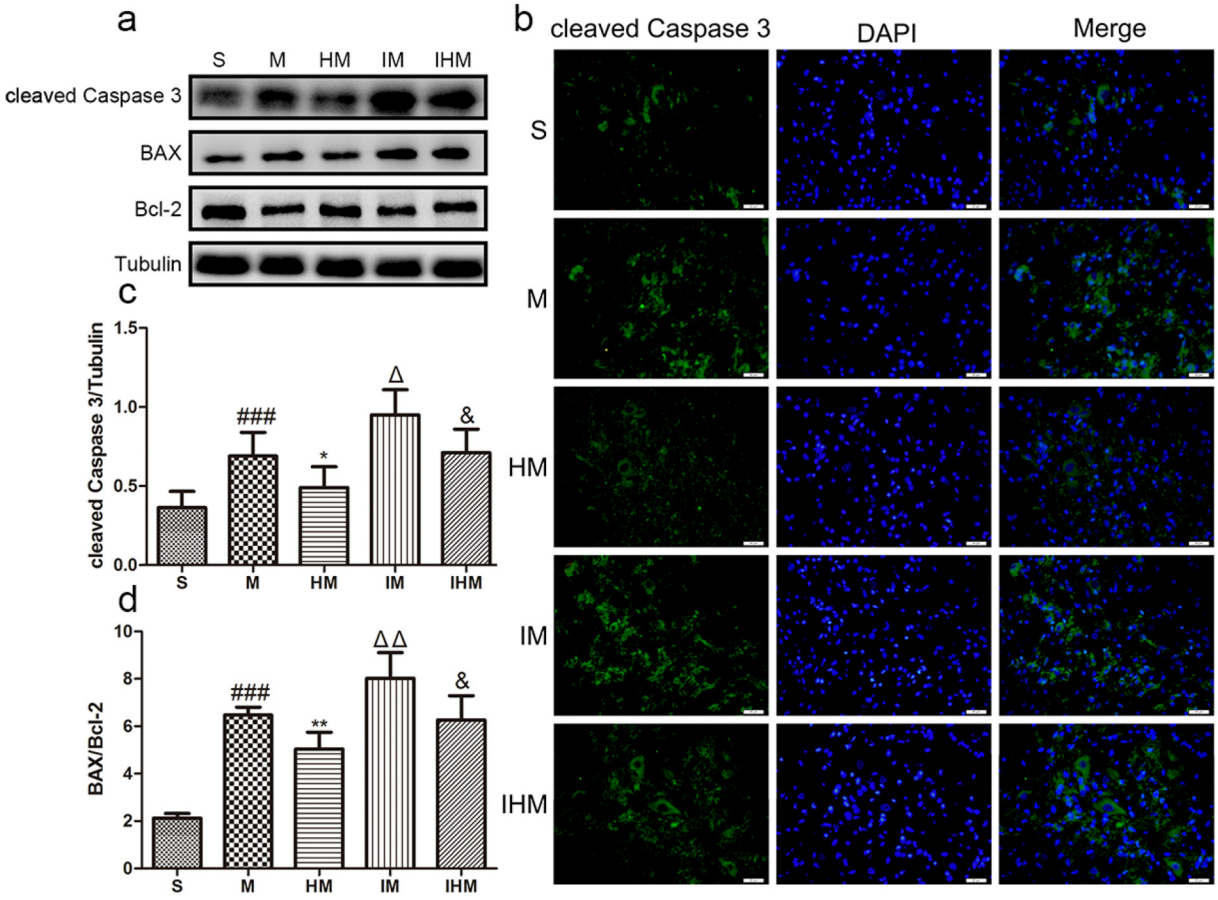

Fig. 5. HBOT promoted the BDNF/TrkB-dependent effect of anti-apoptosis, while inhibitor increased apoptosis caused by SCI. a, c, d Representative western blots and quantification data of cleaved caspase 3, Bax, Bcl-2, and Tubulin in each group. Columns represent mean ± SD, n = 5. $^{\#}p < 0.05$ as M group versus S group, $^{*}p < 0.05$ as HM group versus M group, $^{\triangle}p < 0.05$ as IM group versus M group, $^{\&}p < 0.05$ as IHM group versus HM group. b cleaved Caspase 3 staining in the anterior horn. Green: cleaved Caspase 3; Blue: DAPI. Scale bar, 20 μm. ($^{\#}p$, $^{*}p$, $^{\triangle}p$, $^{\&}p < 0.05$; $^{\#\#}p$, $^{**}p$, $^{\triangle\triangle}p$, $^{\&\&}p < 0.01$; $^{\#\#\#}p$, $^{***}p$, $^{\triangle\triangle\triangle}p$, $^{\&\&\&}p < 0.001$). (For interpretation of the references to colour in this figure legend, the reader is referred to the web version of this article.)

$p = 0.0084$; TrkB mRNA, IM vs M, $p = 0.0090$). In addition, inhibitor can significantly downregulated HBOT-promoted both BDNF and TrkB expression levels by comparing IHM group with HM group. (BDNF, IHM vs HM, $p = 0.015$; TrkB, IHM vs HM, $p = 0.0064$; BDNF mRNA, IHM vs HM, $p = 0.030$; TrkB mRNA, IHM vs HM, $p = 0.020$). These results indicated that HBOT upregulated the BDNF/TrkB signaling pathway following SCI, while inhibitor downregulated the HBOT-dependent BDNF/TrkB signaling pathway.

3.4. HBOT improved the BDNF/TrkB-dependent effects of protectin neurons and anti-apoptosis, while inhibitor had the opposite effects

To test whether HBOT improved the BDNF/TrkB-dependent effect on anti-apoptosis and surviving neurons, the degree of apoptosis was investigated by western blot detecting the levels of cleaved caspase 3, Bax, and Bcl-2 (Fig. 5a, c, d). The expression level of cleaved caspase 3 and the ratio of Bax/Bcl-2 in HM group were lower than these in M group (cleaved caspase 3, HM vs M, $p = 0.011$; Bax/Bcl-2, HM vs M, $p = 0.0072$), and the expression level as well as the ratio in IM group were higher than these in M group (cleaved caspase 3, IM vs M, $p = 0.024$; Bax/Bcl-2, IM vs M, $p = 0.0042$). Meanwhile, compared with HM group, the expression level of cleaved caspase 3 and the ratio of Bax/Bcl-2 in IHM group were significantly increased (cleaved caspase 3, IHM vs HM, $p = 0.020$; Bax/Bcl-2, IHM vs HM, $p = 0.019$). Additionally, the change of cleaved caspase-3 from immunofluorescence was consistent with the trend of cleaved caspase 3 (Fig. 5b).

With the analysis of TUNEL staining, there was a significant decrease of apoptotic cells by comparison HM group with M group (HM vs. M, $p = 0.0019$), while there was a significant increase of apoptotic cells in IM group by comparing with M group (IM vs. M, $p = 0.011$). We further tested the relationship between apoptosis after SCI with HBOT and the BDNF/TrkB signaling pathway. Compared with the HM group, the number of apoptotic cells in the IHM group were significantly increased (IHM vs. HM, $p = 0.0075$) (Fig. 6a, c). Finally, we testified whether HBOT can promoted the BDNF/TrkB- induced effect of surviving neurons. To observe the loss of mature neurons in the anterior horn of T9-T11, we used NeuN/DAPI immunofluorescence labeling (Fig. 6b, d). The number of NeuN/DAPI-positive cell was remarkably higher in the HM group but lower in the IM group than that in the M group (HM vs. M, $p = 0.0019$; IM vs. M, $p = 0.026$). Furthermore, significantly fewer NeuN/DAPI- positive cell in the anterior horn region were found in the IHM group than in the HM group (IHM vs. HM, $p = 0.0016$). All of these results demonstrated that HBOT was an effective therapeutic strategy for inhibiting apoptosis and protecting neurons after SCI, while the BDNF/TrkB signaling pathway can not only mediate neurons protection against apoptosis but also involved in HBOT-mediated neurons protection.

3.5. HBOT inhibited dendritic degeneration by upregulating BDNF/TrkB signaling pathways, while the inhibitor abolished these effects

Because alteration of dendrite in the anterior horn is closely associated with locomotor function, we examined the influence of HBOT on

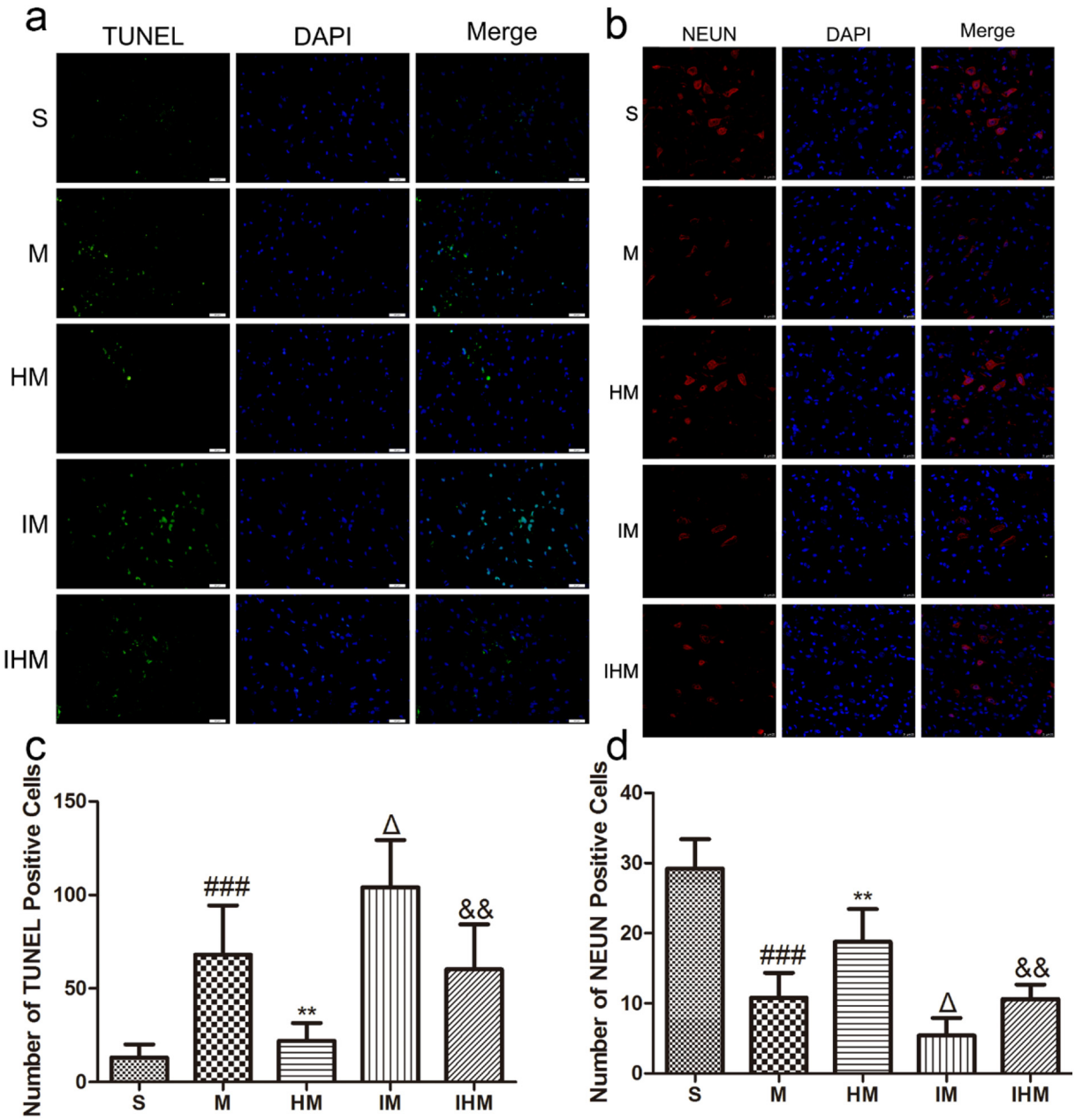

Fig. 6. HBOT improved the BDNF/TrkB-induced effects of decreasing neuronal loss and apoptosis, while inhibitor had the opposite effects. a TUNEL staining in the anterior horn. b NeuN staining in the anterior horn. Red: NeuN; blue: DAPI. Scale bar, 20 μm. c, d Quantitative estimation positive cells. Columns represent mean ± SD, $n = 4$, $^{\#}p < 0.05$ as M group versus S group, $^{*}p < 0.05$ as HM group versus M group, $^{\triangle}p < 0.05$ as IM group versus M group, $^{\&}p < 0.05$ as IHM group versus HM group. ($^{\#}p$, $^{*}p$, $^{\triangle}p$, $^{\&}p < 0.05$; $^{\#\#}p$, $^{**}p$, $^{\triangle\triangle}p$, $^{\&\&}p < 0.01$; $^{\#\#\#}p$, $^{***}p$, $^{\triangle\triangle\triangle}p$, $^{\&\&\&}p < 0.001$). (For interpretation of the references to colour in this figure legend, the reader is referred to the web version of this article.)

total length of dendritic branches and total number of dendrite intersection points based on Golgi-Cox staining. Moreover, MAP-2 has an intimate relationship with SCI and is considered to be an indication of compensatory dendrite reconstruction in remaining neurons. Several studies have revealed that the expression of MAP-2 decreases after SCI. In this study, SCI caused severe damage to dendrites compared with the S group (Figs. 7a, b, c, 8a-g). Compared with the M group, the MAP-2 expression level, total dendrite length and dendrite intersections were significantly higher in the HM group (HM vs. M: MAP-2, $p < 0.001$; total length of dendritic branches, $p = 0.0033$; total number of intersection points, $p = 0.015$), while there were lower MAP-2 expression levels, shorter total dendrite length, and fewer dendrite intersections in the IM group(IM vs. M: MAP-2, $p = 0.0045$; total length of dendritic branches, $p = 0.038$; total number of intersection points, $p = 0.046$). To ascertain the relationship between HBOT-inhibited degeneration of dendrite and the BDNF/TrkB signaling pathway, we further compared the HM group and the IHM group and found that the MAP-2 expression level, total dendrite length and number of dendrite intersections in the IHM group significantly decreased (IHM vs. HM: MAP-2, $p = 0.011$; total length of dendritic branches, $p = 0.022$; total number of intersection points, $p = 0.031$).

3.6. HBOT suppressed damage of dendritic spine and synapse via upregulation of the BDNF/TrkB signaling pathways

After SCI, dendritic spine density of motoneurons in the anterior horn was significantly decreased compared with the S group (Fig. 9e, f). Compared with the M group, dendritic spine density was significantly

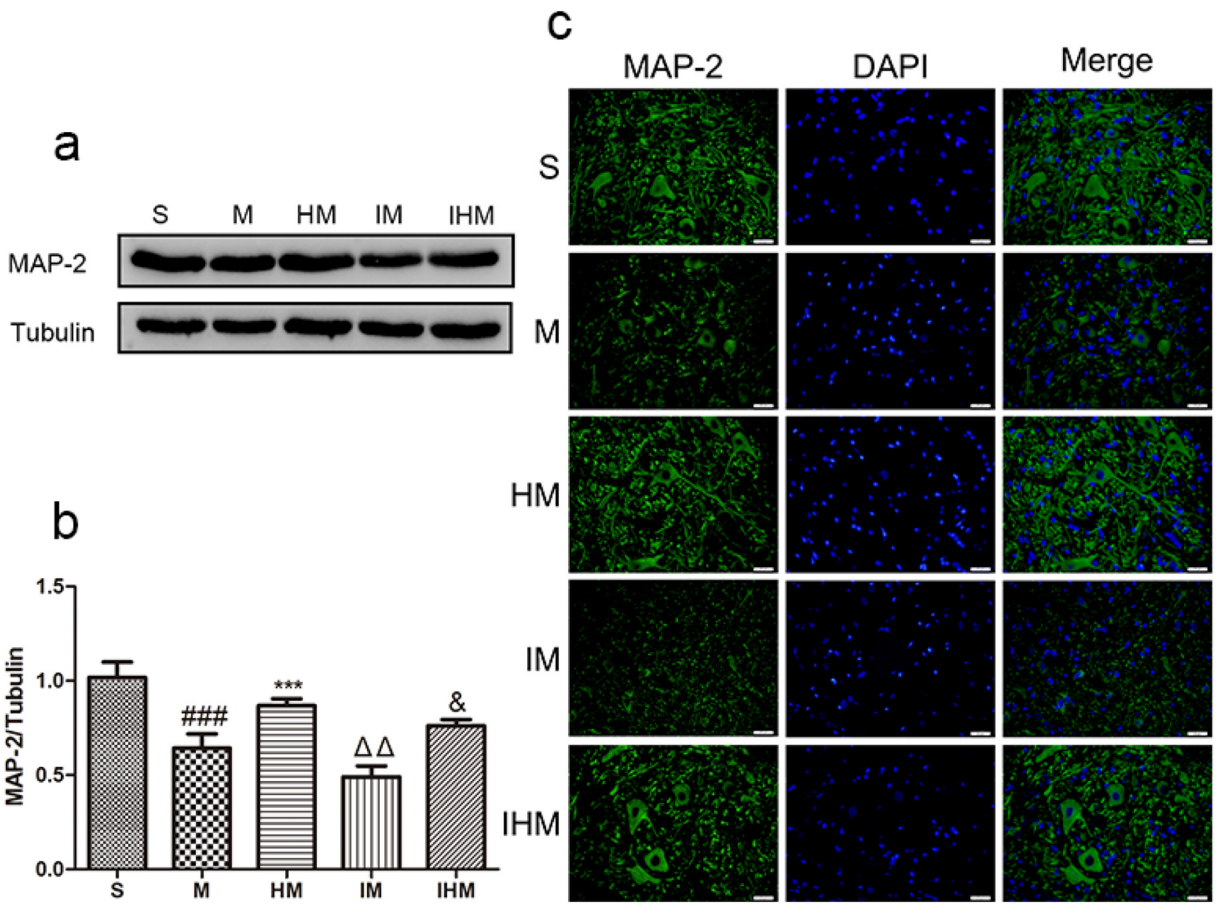

Fig. 7. HBOT increased the MAP-2 expression via upregulating BDNF/TrkB signaling pathways. a, b Represent western blots and quantification data of MAP-2 and Tubulin in each group. Columns represent mean ± SD, $n = 5$. $^{\#}p < 0.05$ as M group versus S group, $^{*}p < 0.05$ as HM group versus M group, $^{\Delta}p < 0.05$ as IM group versus M group, $^{\&}p < 0.05$ as IHM group versus HM group. c MAP-2 staining in the anterior horn. Green: MAP-2; Blue: DAPI. Scale bar, 20 μm. ($^{\#}p$, $^{*}p$, $^{\triangle}p$, $^{\&}p < 0.05$; $^{\#\#}p$, $^{**}p$, $^{\triangle\triangle}p$, $^{\&\&}p < 0.01$; $^{\#\#\#}p$, $^{***}p$, $^{\triangle\triangle\triangle}p$, $^{\&\&\&}p < 0.001$). (For interpretation of the references to colour in this figure legend, the reader is referred to the web version of this article.)

higher in the HM group (HM vs. M, $p = 0.0020$), while there was fewer dendritic spine density in the IM group (IM vs. M, $p = 0.038$). To verify whether HBOT can suppressed damage of dendritic spine via upregulation of the BDNF/TrkB signaling pathways, we compared the dendritic spine density in IHM group with this in HM group and found that the dendritic spine density in the IHM group significantly decreased (IHM vs. HM, $p = 0.0012$).

Western blot and immunofluorescence assays were performed to evaluate the protein level of PSD95. The expression level of PSD95 was significantly decreased in the M group compared with the S group (Fig. 9b, c). Compared with the M group, HBOT significantly restored the PSD95 level (HM vs. M, $p < 0.001$), while the expression of PSD95 in the IM group was remarkably downregulated (IM vs. M, $p = 0.020$). In addition, the expression level of PSD95 in the IHM group was significantly lower than that in the HM group (IHM vs. HM, $p = 0.038$). A similar trend was found for PSD95-positive cells detected by immunofluorescence (Fig. 9a, d). In addition, to determine the deficits of synapse morphology in neurons, we examined synapse morphology by TEM (Fig. 9g). The S group exhibited normal neurons with complete synaptic structures. The M group appeared to exhibit fewer clear and irregular synaptic vesicles and narrower synaptic clefts compared with the HM group, while the IM group exhibited synaptic membranes with more severe uneven thickness, formation of synaptic lysis cavities, and even invisible synaptic connections. Finally, the IHM group exhibited more deficits in synapse morphology than the HM group.

4. Discussion

In this study, we found that HBOT played an important role in the recovery of SCI – attenuating apoptosis, degeneration of dendrite and dendritic spine and synaptic damage of motoneurons in the anterior horn after SCI. Furthermore, the BDNF/TrkB signaling pathway can not only decrease dendritic/synaptic degeneration and reduce apoptosis after SCI but also be involved in the potential molecular mechanism of the HBOT-induced these effects.

SCI caused severe dysfunction, which was followed by spontaneous locomotor functional recovery. This partial recovery may be due to the survival of axons and dendritic as well as the neurotrophic factors expression. In our study, we found that neurons and the dendritic characteristics (the total length of dendritic branches, total number of intersection points and density of dendritic spines) in the M group were significantly decreased. Moreover, there was partial self-recovery in the BBB scores analysis by comparing rats in the M group between 6 h and 7 days after SCI. It can be explained that death is not the only outcome of injured spinal motoneurons, and importantly, remaining motoneurons after injury show a variety of morphological and functional changes. For example, dendritic reorganization and synaptic plasticity. Dendritic and synaptic damage is likely responsible for at least some movement deficits and reduces the excitability of the remaining motoneurons [36,37].

Given that we currently can't replace dead motoneurons, developing the ability to protect motoneurons from injury-induced cell death and secondary injury is an important goal. HBOT increase the oxygen

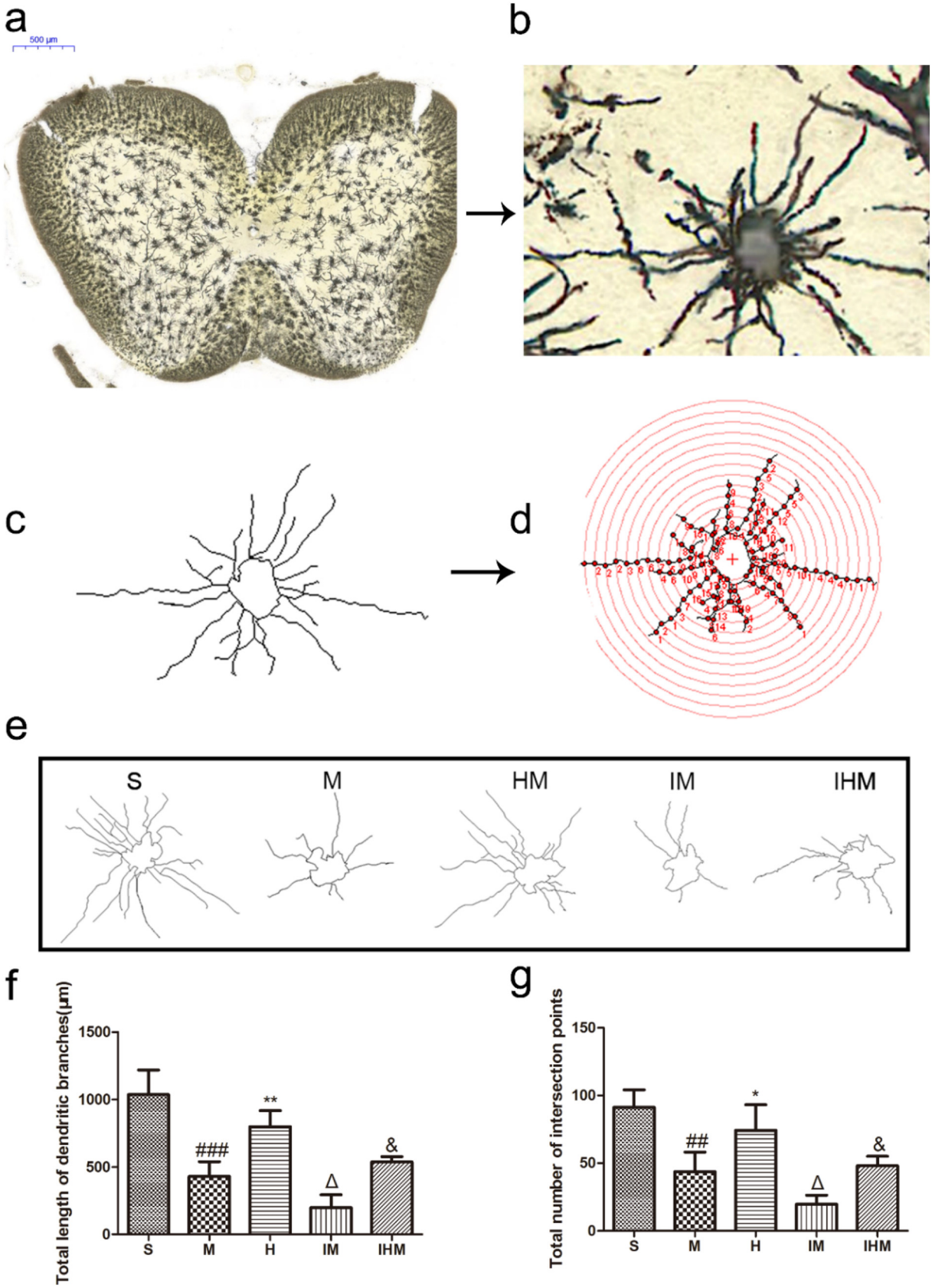

Fig. 8. HBOT inhibited degeneration of dendrite by upregulating BDNF/TrkB signaling pathways. a, b Schematic diagram of the anterior horn. c, d, e Examples of reconstructed neurons and the dendritic characteristics were assessed by Sholl analysis. f The total length of dendritic branches in each group. g Total number of intersection points. Columns represent mean ± SD, $n = 4$. $^{\#}p < 0.05$ as M group versus S group, $^{*}p < 0.05$ as HM group versus M group, $^{\Delta}p < 0.05$ as IM group versus M group, $^{\&}p < 0.05$ as IHM group versus HM group. ($^{\#}p$, $^{*}p$, $^{\Delta}p$, $^{\&}p < 0.05$; $^{\#\#}p$, $^{**}p$, $^{\Delta\Delta}p$, $^{\&\&}p < 0.01$; $^{\#\#\#}p$, $^{***}p$, $^{\Delta\Delta\Delta}p$, $^{\&\&\&}p < 0.001$).

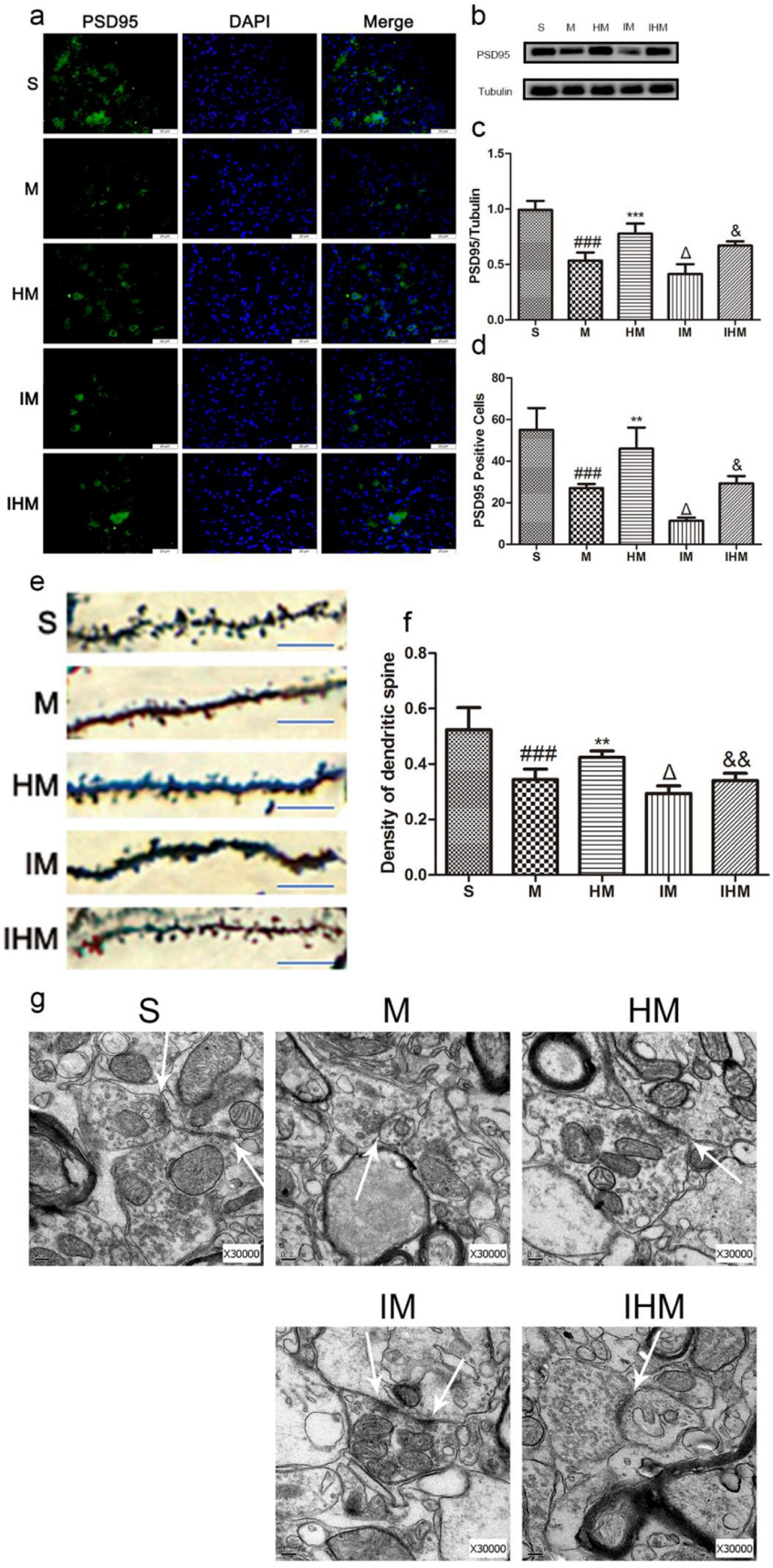

Fig. 9. HBOT suppressed damage of dendritic spine and synapse via upregulation of the BDNF/TrkB signaling pathways, while the inhibitor abolished these effects. a, d PSD95 staining and quantification data of positive cells in the anterior horn. Green: PSD95; Blue: DAPI. Scale bar, 20 μm. Columns represent mean ± SD, n = 4 b, c Represent western blots and quantification data of PSD95 and Tubulin in each group. Columns represent mean ± SD, n = 5 e Examples of dendritic spines. Scale bar, 10 μm. f Density of dendritic spines. Columns represent mean ± SD, n = 4. g Transmission electron microscopy showed the synaptic structures, and the scale bars indicate 0.2 μm. $^{\#}p < 0.05$ as M group versus S group, $^{*}p < 0.05$ as HM group versus M group, $^{\Delta}p < 0.05$ as IM group versus M group, $^{\&}p < 0.05$ as IHM group versus HM group. ($^{\#}p$, $^{*}p$, $^{\triangle}p$, $^{\&}p < 0.05$; $^{\#\#}p$, $^{**}p$, $^{\triangle\triangle}p$, $^{\&\&}p < 0.01$; $^{\#\#\#}p$, $^{***}p$, $^{\triangle\triangle\triangle}p$, $^{\&\&\&}p < 0.001$). (For interpretation of the references to colour in this figure legend, the reader is referred to the web version of this article.)

content in the blood, dilate arterioles, elevate the oxygen diffusion distance, improve local microcirculation, attenuate edema and ischemia/hypoxia. These affects are attributed to the neural protection at the injured site and the reversal of secondary injury to surrounding neurons. Interestingly, we found that HBOT had no significant effects on activating the BDNF/TrkB signaling pathway, as well as BBB scores, tissue structure and protein expression in the S group. Moreover, HBOT couldn't function through the BDNF/TrkB signaling pathway without SCI model. This result can be interpreted as that without SCI, BDNF/TrkB signaling pathway is in an inactive state and the HBOT does not work. In contrast, when SCI occurs, the BDNF/TrkB signaling pathway is activated. Therefore, HBOT/inhibitor can have protective/destructive effect by up/down-regulating BDNF/TrkB signaling pathway, respectively. After SCI, the change of the dendrite and synapse in the anterior horn is the basis for the motor function recovery. In our work, SCI-induced dendrite atrophy and synaptic damage were attenuated by HBOT. Changes of dendrite and synapse would allow them to maintain their connectivity patterns and participate in neural networks in spinal cord. In accordance with functional recovery, the results indicated that HBOT improved motor recovery by suppressing dendrite atrophy and dendritic loss of motoneurons after 7d SCI. As expected, we found that HBOT obviously increased the expression of BDNF and TrkB. BDNF is mainly expressed in neurons and a small number of astrocytes in the early stage of SCI. After SCI, the pathological mechanisms and signaling pathways are complex. We found hyperbaric oxygen therapy significantly increased the BDNF and TrkB expression by comparing with M group. This result might be attributed to the delayed necrotic and/or apoptotic death of the BDNF-producing cells in the spinal anterior neurons after SCI and survival of these BDNF producing cells by the HBOT. These phenomena were also observed in our experiment when we analyzed apoptosis and surviving neurons.

Activation of BDNF/TrkB signal pathway after spinal cord injury can anti-apoptosis and promote the survival of damaged neurons. In addition, BDNF/TrkB can promote the axon and dendritic sprouting of adult neurons, enhance the release of synaptic transmitters and strengthen the intersynaptic signal transduction. In this experiment, we further demonstrated this view by administering pathway-specific inhibitor. In preliminary results, the inhibitor (ANA-12) couldn't affect neurological function and had no significant effects on synapse and dendrite of rats without SCI. This result excluded the possibility that the inhibitor itself may affect neurological function. Results from Golgi staining indicated that inhibitor could decrease the dendritic length, complexity and spine density after SCI. These results demonstrated that the BDNF/TrkB pathway was essential to maintenance of dendrite and synapse as well as anti-apoptosis after SCI.

The degeneration and reorganization of dendritic spines is a complicated process and could be regulated through multiple mechanisms, including receptors, scaffolding proteins, and regulators of the cytoskeleton [38]. Somatically synthesized BDNF promoted spine formation, whereas dendritically synthesized BDNF was a key regulator of spine head growth and spine pruning in rat hippocampal neuronal cultures [39]. This result indicated that the BDNF/TrkB signal pathway can directly participate in the formation, maturation, and pruning of dendritic spines. However, the BDNF/TrkB pathway exerts its effects through multiple mechanisms in vivo, such as promote neurogenesis and angiogenesis. In the central nervous system, neurovascular regeneration is tightly associated with neural plasticity. BDNF/TrkB pathway may indirectly promote dendritic plasticity and synapse formation by improving angiogenesis and neurogenesis. Therefore, our experiment only can prove that the BDNF/TrkB signal pathway is related to dendritic growth and synapse formation after SCI. However, it can't demonstrate whether the BDNF/TrkB pathway directly or indirectly mediates dendritic、dendritic spine and synaptic changes.

We further analyzed the relationship between HBOT-induced effects (anti-apoptosis, reduction degeneration of dendrite and synapse) and the BDNF/TrkB signaling pathway. A significantly shorter total dendritic length, intersection points and lower spine density as well as larger neuron loss were observed in the IHM group when compared by HM group, same as the lower expression levels of BDNF and TrkB. These results indicated that HBOT decreased dendritic/synaptic degeneration and alleviated apoptosis after SCI through BDNF/TrkB signaling pathway. Our experiment only observed changes in dendrite/synapse and apoptosis after 7d HBOT following SCI. The expression of BDNF is in dynamic changes after spinal cord injury. In the late stage of SCI, whether hyperbaric oxygen therapy still has effects on anti-apoptosis and reducing dendritic/synaptic degeneration and whether it can play the same role in the late stage through BDNF/TrkB signaling pathway requires further research.

There are major limitations in this study. First, we only established a 7-day time point and could not evaluate the long-term effects of hyperbaric oxygen therapy or the BDNF/TrkB pathway after SCI. Second, this study only discussed changes in the density and structure of neurons in the anterior horn after SCI. Because of the experimental conditions, we couldn't use electrophysiological technology to observe the change in LTP and LTD at the functional level. Third, there was no deeper study of downstream molecular changes in the BDNF/TrkB signaling pathway. It was not definitely demonstrated whether hyperbaric oxygen therapy increased the BDNF and TrkB directly or indirectly.

5. Conclusion

HBOT plays a novel role in the recovery of SCI by decreasing apoptosis and suppressing dendritic/synaptic degeneration in the anterior horn after SCI. Furthermore, the BDNF/TrkB signaling pathways have positive effects on anti-apoptosis and suppressing dendritic/synaptic degeneration. Additionally, HBOT reduces apoptosis and attenuates degeneration of dendrite and synapse via upregulating BDNF/TrkB signaling pathways.

Funding statement

The work presented in this manuscript was supported by the Foundation of Health Committee of Zhejiang province, China (No. 2017KY482). The authors thank the other researchers for the valuable technical assistance in this work.

Declaration of Competing Interest

The authors declare that there are no competing interests.

References

[1] M. Cordaro, et al., Fumaric acid esters attenuate secondary degeneration after spinal cord injury, J. Neurotrauma 34 (21) (2017) 3027–3040.
[2] D. Zhang, et al., Metformin improves functional recovery after spinal cord injury via autophagy flux stimulation, Mol. Neurobiol. 54 (5) (2017) 3327–3341.
[3] T. Bhatnagar, et al., Quantifying the internal deformation of the rodent spinal cord during acute spinal cord injury - the validation of a method, Comput. Methods Biomech. Biomed. Engin. 19 (4) (2016) 386–395.
[4] J. Rao, R. Tiruchelvarayan, L. Lee, Palliative surgery for cervical spine metastasis, Singap. Med. J. (2014 Nov) 569–573 [cited 55 11]; 2015/01/30.
[5] C. Rouanet, et al., Traumatic spinal cord injury: current concepts and treatment update, Arq. Neuropsiquiatr. 75 (6) (2017) 387–393.
[6] J. Gu, J.Q. Zheng, Microtubules in dendritic spine development and plasticity, Open Neurosci. J. 3 (2009) 128–133.
[7] E.P. Buen, et al., Spinogenesis and plastic changes in the dendritic spines of spinal cord motoneurons after traumatic injury in rats, Arch. Med. Res. 48 (7) (2017) 609–615.
[8] S.P. Bandaru, et al., Dendritic spine dysgenesis contributes to hyperreflexia after spinal cord injury, J. Neurophysiol. 113 (5) (2015) 1598–1615.
[9] Y. Li, et al., Neuronal damage and plasticity identified by microtubule-associated protein 2, growth-associated protein 43, and cyclin D1 immunoreactivity after focal cerebral ischemia in rats, Stroke 29 (9) (1998) 1972–1980 (discussion 1980-1).
[10] Gonzalez-Tapia, D., et al., The motor learning induces plastic changes in dendritic spines of Purkinje cells from the neocerebellar cortex of the rat. 2015. Restor. Neurol. Neurosci.33(5): p. 639–45.

[11] P.D. Ganzer, et al., Serotonin receptor and dendritic plasticity in the spinal cord mediated by chronic serotonergic pharmacotherapy combined with exercise following complete SCI in the adult rat, Exp. Neurol. 304 (2018) 132–142.
[12] D.R. Sengelaub, X.M. Xu, Protective effects of gonadal hormones on spinal motoneurons following spinal cord injury, Neural Regen. Res. 13 (6) (2018) 971–976.
[13] J.W. Tan, et al., Hyperbaric oxygen ameliorated the lesion scope and nerve function in acute spinal cord injury patients: a retrospective study, Clin. Biochem. 53 (2018) 1–7.
[14] N.P. Patel, J.H. Huang, Hyperbaric oxygen therapy of spinal cord injury, Med. Gas Res. 7 (2) (2017) 133–143.
[15] B. Zhao, et al., Hyperbaric oxygen pretreatment improves cognition and reduces hippocampal damage via p38 mitogen-activated protein kinase in a rat model, Yonsei Med. J. 58 (1) (2017) 131–138.
[16] Y. Long, et al., Hyperbaric oxygen therapy reduces apoptosis after spinal cord injury in rats, Int. J. Clin. Exp. Med. 7 (11) (2014) 4073–4081.
[17] P.A. Tai, et al., Attenuating experimental spinal cord injury by hyperbaric oxygen: stimulating production of vasculoendothelial and glial cell line-derived neurotrophic growth factors and interleukin-10, J. Neurotrauma 27 (6) (2010) 1121–1127.
[18] N. Weishaupt, A. Blesch, K. Fouad, BDNF: the career of a multifaceted neurotrophin in spinal cord injury, Exp. Neurol. 238 (2) (2012) 254–264.
[19] W. Chou, et al., Exercise rehabilitation attenuates cognitive deficits in rats with traumatic brain injury by stimulating the cerebral HSP20/BDNF/TrkB signalling axis, Mol. Neurobiol. 55 (11) (2018) 8602–8611.
[20] C.B. Mantilla, et al., Motoneuron BDNF/TrkB signaling enhances functional recovery after cervical spinal cord injury, Exp. Neurol. 247 (2013) 101–109.
[21] B. Wang, Y. Li, Panax notoginseng saponins improve recovery after spinal cord transection by upregulating neurotrophic factors, Neural Regen. Res. 10 (8) (2015) 1317–1320.
[22] E. Edelmann, et al., Theta burst firing recruits BDNF release and signaling in postsynaptic CA1 neurons in spike-timing-dependent LTP, Neuron 86 (4) (2015) 1041–1054.
[23] T.V. Bliss, T. Lomo, Long-lasting potentiation of synaptic transmission in the dentate area of the anaesthetized rabbit following stimulation of the perforant path, J. Physiol. 232 (2) (1973) 331–356.
[24] G. Leal, P.M. Afonso, C.B. Duarte, Neuronal activity induces synaptic delivery of hnRNP A2/B1 by a BDNF-dependent mechanism in cultured hippocampal neurons, PLoS One 9 (10) (2014) e108175.
[25] Z. Ying, et al., BDNF-exercise interactions in the recovery of symmetrical stepping after a cervical hemisection in rats, Neuroscience 155 (4) (2008) 1070–1078.
[26] H. Wang, et al., Treadmill training induced lumbar motoneuron dendritic plasticity and behavior recovery in adult rats after a thoracic contusive spinal cord injury, Exp. Neurol. 271 (2015) 368–378.
[27] P. Xing, et al., The protection effect and mechanism of hyperbaric oxygen therapy in rat brain with traumatic injury, Acta Cir. Bras. 33 (4) (2018) 341–353.
[28] Y. Sun, et al., Changes in autophagy in rats after spinal cord injury and the effect of hyperbaric oxygen on autophagy, Neurosci. Lett. 618 (2016) 139–145.
[29] X. Liu, et al., Hyperbaric oxygen treatment protects against spinal cord injury by inhibiting endoplasmic reticulum stress in rats, Spine (Phila Pa 1976) 40 (24) (2015) E1276–E1283.
[30] L. Chen, et al., The small-molecule TrkB agonist 7, 8-dihydroxyflavone decreases hippocampal newborn neuron death after traumatic brain injury, J. Neuropathol. Exp. Neurol. 74 (6) (2015) 557–567.
[31] H.Y. Zhang, et al., Regulation of autophagy and ubiquitinated protein accumulation by bFGF promotes functional recovery and neural protection in a rat model of spinal cord injury, Mol. Neurobiol. 48 (3) (2013) 452–464.
[32] L. Zhang, et al., Physical exercise improves functional recovery through mitigation of autophagy, attenuation of apoptosis and enhancement of neurogenesis after MCAO in rats, BMC Neurosci. 14 (2013) 46.
[33] D.A. Sholl, Dendritic organization in the neurons of the visual and motor cortices of the cat, J. Anat. 87 (4) (1953) 387–406.
[34] R.L. Gibb, et al., Tactile stimulation promotes motor recovery following cortical injury in adult rats, Behav. Brain Res. 214 (1) (2010) 102–107.
[35] O. Hurtado, et al., A chronic treatment with CDP-choline improves functional recovery and increases neuronal plasticity after experimental stroke, Neurobiol. Dis. 26 (1) (2007) 105–111.
[36] J.J. Bernstein, N.A. Standler, Dendritic alteration of rat spinal motoneurons after dorsal horn mince: computer reconstruction of dendritic fields, Exp. Neurol. 82 (3) (1983) 532–540.
[37] C.M. Little, K.D. Coons, D.R. Sengelaub, Neuroprotective effects of testosterone on the morphology and function of somatic motoneurons following the death of neighboring motoneurons, J. Comp. Neurol. 512 (3) (2009) 359–372.
[38] T. Tada, M. Sheng, Molecular mechanisms of dendritic spine morphogenesis, Curr. Opin. Neurobiol. 16 (1) (2006) 95–101.
[39] L.L. Orefice, et al., Distinct roles for somatically and dendritically synthesized brain-derived neurotrophic factor in morphogenesis of dendritic spines, J. Neurosci. 33 (28) (2013) 11618–11632.